Towards a 10 μs, thin and high resolution pixelated CMOS sensor system for future vertex detectors

R.De Masi[a], S.Amar-Youcef[c], J.Baudot[a], G.Bertolone[a], A.Brogna[a], G.Claus[a], C.Colledani[a], Y.Degerli[b], M.Deveaux[c], A.Dorokhov[a], G.Doziére[a], W.Dulinski[a], M.Gelin[b], M.Goffe[a], J.C.Fontaine[a], Ch.Hu-Guo[a], A.Himmi[a], K.Jaaskelainen[a], M.Koziel[a], F.Morel[a], C.Müntz[c], F.Orsini[b], C.Santos[a], C.Schrader[c], M.Specht[a], J.Stroth[c], I.Valin[a], G.Voutsinas[a], F.M.Wagner[d], M.Winter[a]

[a] *IPHC/IN2P3/CNRS and Université de Strasbourg, Strasbourg, France*
[b] *IRFU / SEDI (CEA) Saclay, France*
[c] *IFK, Goethe-Universität, Frankfurt am Main, Germany*
[d] *Forschungsneutronenquelle Heinz Maier-Leibnitz (FRM II), Technische Universität München, Garching, Germany*

Abstract

The physics goals of many high energy experiments require a precise determination of decay vertices, imposing severe constraints on vertex detectors (readout speed, granularity, material budget, ...). The IPHC-IRFU collaboration developed a sensor architecture to comply with these requirements. The first full scale CMOS sensor was realised and equips the reference planes of the EUDET beam telescope. Its architecture is being adapted to the needs of the STAR (RHIC) and CBM (FAIR) experiments. It is a promising candidate for the ILC experiments and the ALICE detector upgrade (LHC). A substantial improvement to the CMOS sensor performances, especially in terms of radiation hardness, should come from a new fabrication technology with depleted sensitive volume. A prototype sensor was fabricated to explore the benefits of the technology. The crucial system integration issue is also currently being addressed. In 2009 the PLUME collaboration was set up to investigate the feasibility and performances of a light double sided ladder equipped with CMOS sensors, aimed primarily for the ILC vertex detector but also of interest for other applications such as the CBM vertex detector.

Key words: CMOS, vertex detector, system integration

---

1. Introduction

The development of CMOS sensors for high energy applications was driven by the project of a vertex detector for the International Linear Collider (ILC) experiments [1]. Physics goals and running conditions impose stringent requirements on this detector: single point resolution below 3 μm, material budget of about $0.1-0.2\%$ X_0 per ladder, integration time ranging from 25 to 100 μs, depending on the distance of the sensitive layer from the interaction point. This is in order to achieve a resolution on the impact parameter $\sigma \ \leq \ 5\ \mu m \oplus 10\ \mu m \cdot GeV/p \sin^{3/2}\theta$, far better of what was achieved up to now by any vertex detector, which is essential for the precise measurements the ILC is aiming for. Furthermore the sensors have to withstand a dose of about 0.3 $MRad$ and a fluence of few 10^{11} n_{eq}/cm^2 within five years, and the total power dissipated should remain well below 100 W to comply with passive cooling. For the ILD detector [2], two possible geometries are presently under study: one with five single-sided layers of sensors and a second one, technologically more ambitious, with three layers equipped with sensors on both sides, 2 mm apart.

2. CMOS pixel sensors

As compared with other pixel technologies, CMOS sensors are particularly attractive for high precision devices. As for any silicon based sensor, the signal generated by a charged particle traversing a CMOS sensor is due to the electron-hole pairs created in the sensitive volume, which has a low resistivity. The sensitive thickness of CMOS sensors is typically $10-20$ μm, which translates into ~ 1000 e^- created by a minimum ionising particle, typically collected on a 3×3 pixels cluster. The charge carriers propagate thermally and are collected by the sensing diodes formed by n-wells in contact with the p-type substrate.

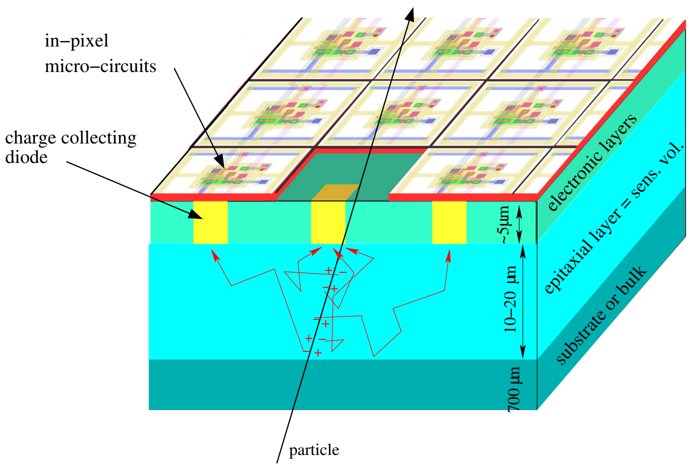

Figure 1: Principle of operation of a CMOS sensor.

This detection principle is illustrated in Fig. 1. The intrinsic advantages of this technology come from the extremely high granularity (down to few microns), the small thickness (few tens of microns) and the signal processing micro-circuits integrated on the sensor substrate. But they are at the expense of moderate radiation tolerance and intrinsic speed. Additionally, the small signal per pixel calls for a low noise read-out electronics. Furthermore, since the n-wells are used to collect the charge, the in-pixel micro-circuitry relies mainly on NMOS transistors.

Driven by subatomic physics applications, within the last 10 years more than 30 sensor prototypes of the MIMOSA series[1] have been designed and produced, with an extensive use of the 0.35 μm OPTO technology. They have been tested both in the laboratory and on high energy beams (from several to 100 GeV). They have a typical noise of $\sim$ 10 e^- which translates into a signal-to-noise ratio (S/N) most probable value between 15 and 30. The detection efficiency is nearly 100% for a fake hit rate per pixel below 10^{-4}. The spatial resolution ranges from 1 to 5 μm, depending on the pitch and on the granularity of the charge encoding. The sensors can tolerate a dose of up to 1 MRad. The tolerance to non-ionising radiation depends on the pitch: a sensor with a 10 μm pitch can stand a fluence of 10^{13} n_{eq}/cm^2, that becomes $2 \cdot 10^{12}$ n_{eq}/cm^2 for 20 μm pitch. The sensors can be operated at temperatures as high as $+40^o$.

MIMOSA sensors have been used in beam telescopes and vertex detector demonstrators [3]. These sensors deliver unfiltered analog outputs and have a typical readout speed of 1 $kFrame/s$ which is inadequate for certain applications.

3. MIMOSA-26

In order to increase the readout frequency, a binary output architecture with column parallel readout was developed in the last years, that allows to read up to 10 kFrame/s. The first full-scale sensor with this architecture, called MIMOSA-26 [4], was produced. The chip is organised in 1152 columns of 576 pixels, each hosting the micro-circuitry to perform a preamplification and correlated double sampling. Each column is terminated with a discriminator and they are read out in parallel. The discriminated signals are processed through a zero-suppression circuitry integrated in the chip. The sensor has an active area of 10.6×21.2 mm^2 for a pixel pitch of 18.4 μm. The average power dissipated is 280 mW/cm^2. The chip was validated in the laboratory and its performances were as expected from the experience with previous prototypes. In order to fully characterise the sensor, a test beam campaign was carried out at the CERN-SPS with a 120 GeV pion beam. Preliminary results are show in Fig. 2. An efficiency of $\sim$ 99.5% and a fake hit rate of about 10^{-4} for a discriminator threshold equal to six times the noise value were observed. The residuals are compatible with the expected resolution of 4 μm.

MIMOSA-26 has been realised in the framework of the EUDET-FP6 project [5], to equip the reference planes of a beam telescope, but its architecture constitutes also the starting point

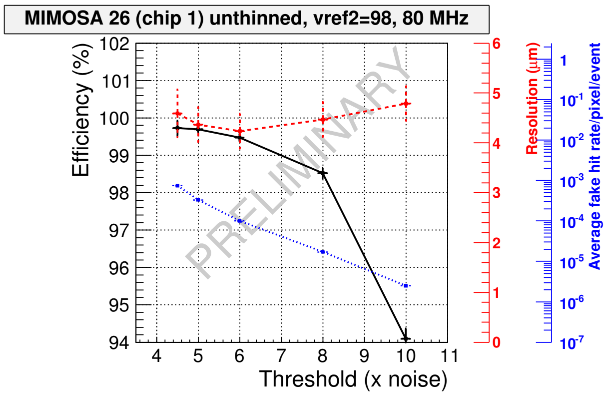

Figure 2: Preliminary results of MIMOSA-26 with 120 GeV pion beam. The efficiency (black curve), average fake hit rate (blue curve) and resolution (red curve) are shown as function of the discriminator threshold in units of noise.

for the development of future sensors. An extended version of this sensor will equip the Heavy Flavour Tracker (HFT) of the STAR experiment [6] at RHIC, in two stages. A first chip, called PHASE-1, currently under test at LBNL, will equip 30% of the detector. The chip has 640 μs readout time, 30 μm pitch, an active area of 4 cm^2 and a binary output. The final sensor, called ULTIMATE, will be faster ($\sim$ 200 μs readout time), more granular (18.4 μm pixel pitch), and with integrated zero-suppression. The final detector is expected to take the first charm data in 2013-2014. MIMOSA-26 provides also the sensor architecture for the Micro Vertex Detector (MVD) of the CBM experiment [7] at FAIR. In this case a faster and more radiation tolerant sensor is needed, since the detector will be exposed to up to 1 $MRad$ and 10^{13} n_{eq}/cm^2 per data taking campaign. Recently this type of sensor has been identified by the ALICE collaboration as of interest for a future upgrade.

MIMOSA 26 is a good forerunner of a sensor matching the requirements for a linear collider vertex detector (VXD), as outlined in Sec.1. A general improvement to the sensor performances will come from reducing the feature size from the present 0.35 μm to 0.18 μm or even less, with additional metal layers as a benefit. A prototype sensor in 0.18 μm technology is presently being designed and will be submitted soon. For the outer layers of the VXD the extension of MIMOSA-26 is almost immediate. The beam background rather moderate and the tracks in a jet quite separated, a pitch of about 35 μm can be sufficient to comply with the expected detector performances. This allows to read out a 2 cm long sensor in about 100 μs or less. In order to provide the required spacial resolution of 3 μm with such a pitch, the discriminators at the end of the column need to be replaced by a 4-5 bits ADC. Two different ADC architectures have been developed; they will be implemented in a sensor and tested by 2011. For the inner layers of the VXD a higher granularity and a faster readout are needed to separate neighbouring tracks in a jet and cope with the higher levels of beam background. A $\lesssim$ 15 μm pitch will insure the aimed spatial resolution also with a binary readout. A faster readout speed will be obtained by reading out the sensor from both sides and moving to smaller feature size. A readout time

[1] standing for Minimum Ionising particle MOS Active pixel sensor.

of 35 – 40 μs seems achievable in this way. Further improvements in the readout speed could come by exploiting the double layer structure, as described in the next section.

4. System integration studies

Another important issue for the ILD vertex detector is the material budget, which needs to be kept down to a few per mill X_0 per layer. The PLUME [8] collaboration is developing a Pixelated Ladder with Ultra-low Material Embedding for this purpose. The goal of the project is to construct a double sided ladder equipped with 6 MIMOSA-26 sensors ($\leq$ 0.3% X_0) on each side to explore the feasibility, the performances and the added value of double sided structures. A major motivation for this developments is the ILD Detector Baseline Document of 2012. Other applications are considered as well. Fig. 3 displays the PLUME ladder concept.

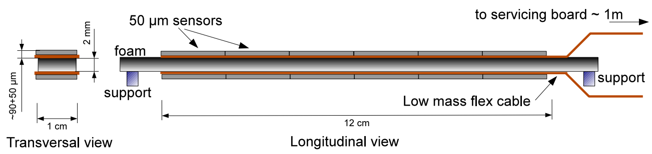

Figure 3: The PLUME ladder: 2×6 MIMOSA-26 sensors thinned down to 50 μm, plus low mass flex cables and foam support. The expected material budget is $\approx 0.2 - 0.3\%$ X_0.

One added value of double sided ladders compared to single sided ones could be an improved time resolution if one side of the ladder is equipped with rectangular pixels, with their longer side along the readout direction. Increasing the pitch size in this direction implies a reduction of the number of rows to be read out; thus the sensor will be faster without changing the sensitive area. These sensors should provide a sort of timestamp to the hits on the innermost layers, which will have the same spatial resolution on both directions. By implementing those rectangular pixels on sensors with depleted epitaxial layer (see next section), a 10 μs time resolution may be achieved. A first, reduced scale prototype, with 2 squared pixel sensors on each layer, has been realised and tested in November 2009 at the CERN-SPS. The PLUME ladder will also be used to study the impact of multi-ladders alignment in the overall track reconstruction, the effect of air-flow cooling on the mechanical stability of the ladder, and the compliance with power cycling in a 3.5 T magnetic field. It could eventually be tested with the infrastructure foreseen in the FP7 AIDA project [9].

Another system integration project under study is SERWIETE, which stays for SEnsor Row Wrapped In an Extra-Thin Envelope, in the framework of the FP7 Hadron Physics 2 project [10]. The latter is exploring the feasibility of supportless ladders by embedding the sensors in thin polymerised films, with the aim of reducing the material budget down to 0.15% X_0 per ladder. This structure is versatile and flexible and may match cylindrical surfaces, such as beam pipes.

5. Further developments

Besides developing fast readout architectures, the IPHC is involved in a R&D line exploiting a new process featuring a high resistivity epitaxial layer ($10^2 - 10^3$ $\Omega \cdot cm$). In this case, with voltages of 4 – 5 V, the depleted depth reaches several microns, to be compared with a fraction of micron in low resistivity epitaxial layers. The charge is thus collected faster, therefore increasing the readout speed; the path length of the charge carriers is shortened, reducing the probability of recombination with free charge carriers, thus improving substantially the tolerance to non ionising radiation. For the same reason the total charge released by impinging particles is collected in fewer pixels which, therefore, exhibit a larger S/N. The charge collection efficiency is also improved, thus allowing for sensors with larger pitch.

The technology was prototyped with a sensor called MIMOSA-25, in a 0.6 μm technology featuring a $\sim$ 14 μm epitaxial layer. The sensor has been tested in the laboratory with a ^{106}Ru β source, and with a 120 GeV pion beam at the CERN-SPS. The average charge collected in the seed pixel is nearly three times larger than in sensors with low resistivity epitaxial layer. The charge is almost fully collected in average on a 2×2 pixels cluster, instead of a 3×3 pixel cluster for undepleted sensors. Fig. 4 shows the S/N distribution for the seed pixel in sensors with a 20 μm pitch before irradiation (black curve) and after a fluence of $3 \cdot 10^{13}$ n_{eq}/cm^2 (red curve). The plots show that even after such a fluence the S/N most probable value is about 30, and the detection efficiency remains close to 100%. These results indicate that high resistivity epitaxial layer technologies will improve the radiation tolerance of the sensors by about two orders of magnitude with respect to standard ones.

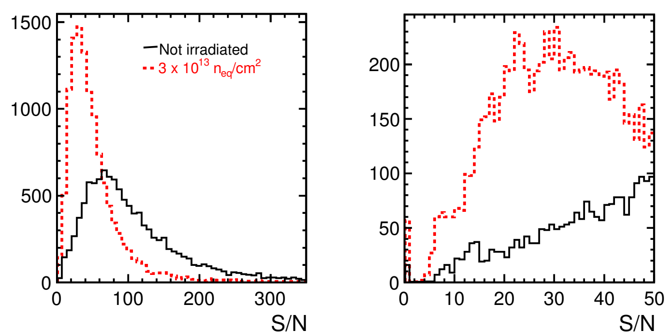

Figure 4: S/N for MIMOSA-25 sensor with a 20 μm pitch before irradiation (black curve) and after a fluence of $3 \cdot 10^{13}$ n_{eq}/cm^2 (red curve). The rigth plot is a zoomed view of the left one.

The MIMOSA-26 sensor has been duplicated with a high resistivity epitaxial layer ($\sim$ 400 $\Omega \cdot cm$) in 0.35 μm technology and it is presently being tested in the laboratory with a ^{106}Ru β source. In order to characterise the sensor, it has been operated in test mode, which allows to read out groups of 8 columns in analogue mode at the reduced frequency of 20 MHz. The preliminary results shown in Fig. 5 indicate that the charge collected on the seed pixel is about twice larger than with a standard epitaxial layer, while the noise stays nearly unchanged.

This is expected to significantly improve the tolerance to non-ionising radiation. The high resistivity epitaxial layer version of MIMOSA-26, irradiated at different fluences, will be tested on beam during summer 2010. The results could greatly benefit to the design of the final sensor for the STAR-HFT.

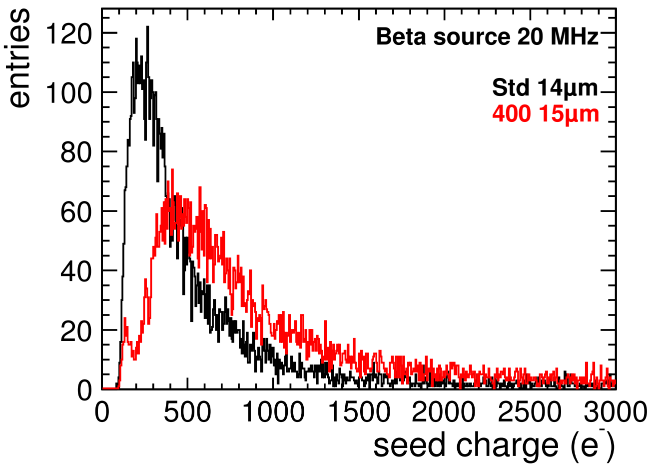

Figure 5: Charge collected on the seed pixel for MIMOSA-26 sensor with standard (low resistivity) 14 μm thin epitaxial layer (black curve) and with high resistivity 15 μm thin epitaxial layer (red curve).

A still different technology with a high resistivity sensitive volume is also under study, in a collaboration led by CERN, in view of the upgrade of detectors for super-LHC. This technology features no epitaxial layer, but offers the advantage of a high resistivity substrate, which may be depleted deeply enough to generate a large signal and to allow for a sizable pixel pitch without detection efficiency losses.

The most promising CMOS sensor R&D line is offered by $3D$ integration techniques, where layers (tiers) with different functionalities, are stapled together and connected through vias at the pixel level. As compared to the standard planar technology, the $3D$ approach expands strongly the in-pixel functionalities. Moreover, different technologies can be combined, selecting the one most adapted for the layer's purpose (sensitive volume, analog readout, digital processing, etc.). The approach is still emerging and needs to be assessed, especially as far as material budget and power dissipation are concerned. Within a consortium led by FERMILAB, different MIMOSA-like prototypes have been submitted for fabrication, which try to combine high level signal processing with low power dissipation [11].

6. Summary

CMOS sensors are now mature to be used in real scale detectors, especially were high resolution and low material budget are needed. MIMOSA sensors are presently equipping beam telescopes and demonstrators of future vertex detectors. A first full scale sensor, called MIMOSA 26, with column-parallel architecture and integrated zero-suppression has been developed to improve the typical readout speed by one order of magnitude to achieve 10^4 $frames/s$. It presently equips the six reference planes of the EUDET beam telescope and it will be further adapted to match the requirements of future vertex detectors (STAR-HFT, ILD, CBM-MVD, ...). In order to maintain the high performances of the sensors when incorporated in a complete detector, the integration issues have to be carefully addressed. Two projects, PLUME and SERWIETE, are studying the possibility to achieve the ambitioned low material budget (few per mill X_0) support structures as well as the impact of cooling, alignment, power cycling, etc. on the track reconstruction. The tolerance to non-ionising radiation, which is modest for a typical CMOS detector, can be improved by about two orders of magnitude by exploiting recently available technologies featuring a depleted epitaxial layer. Preliminary test results obtained with such technologies are very promising. The performances of CMOS sensors are expected to still substantially improve with the help of $3D$ integration technologies. They yet need to be validated but they may be the basis of second generation sensors in view, for example, of the ILC 1 TeV upgrade.

References

[1] R. Turchetta *et* al., Nucl. Instr. and Meth. A 458 (2001) 677.
[2] The ILD Letter of Intent, http://www.ilcild.org/documents/ild-letter-of-intent/LOI.pdf .
[3] M. Winter *et* al., ILC Vertex Detector Review for ALCPG-07, http://www.iphc.cnrs.fr/Others,116.html .
[4] C. Hu-Guo *et* al., Proceedings of the TIPP-09 conference, DOI: 10.1016/j.nima.2010.03.043
[5] EUDET collaboration (EU-FP6), http://www.eudet.org .
[6] L. Greiner *et al.*, Proceedings of PIXEL 2008 Workshop, JINST 4 (2009) P03008.
[7] M. Winter *et al.*, GSI scientific report 2008, Instruments-Methods-11 (2009)
[8] http://www.iphc.cnrs.fr/IMG/memoPLUME_3.pdf .
[9] https://espace.cern.ch/aida/default.aspx .
[10] http://www.hadronphysics2.eu/
[11] R. Yarema, PoS(Vertex 2007)017.